Daniele Struppa
Jeff Tollaksen *Editors*

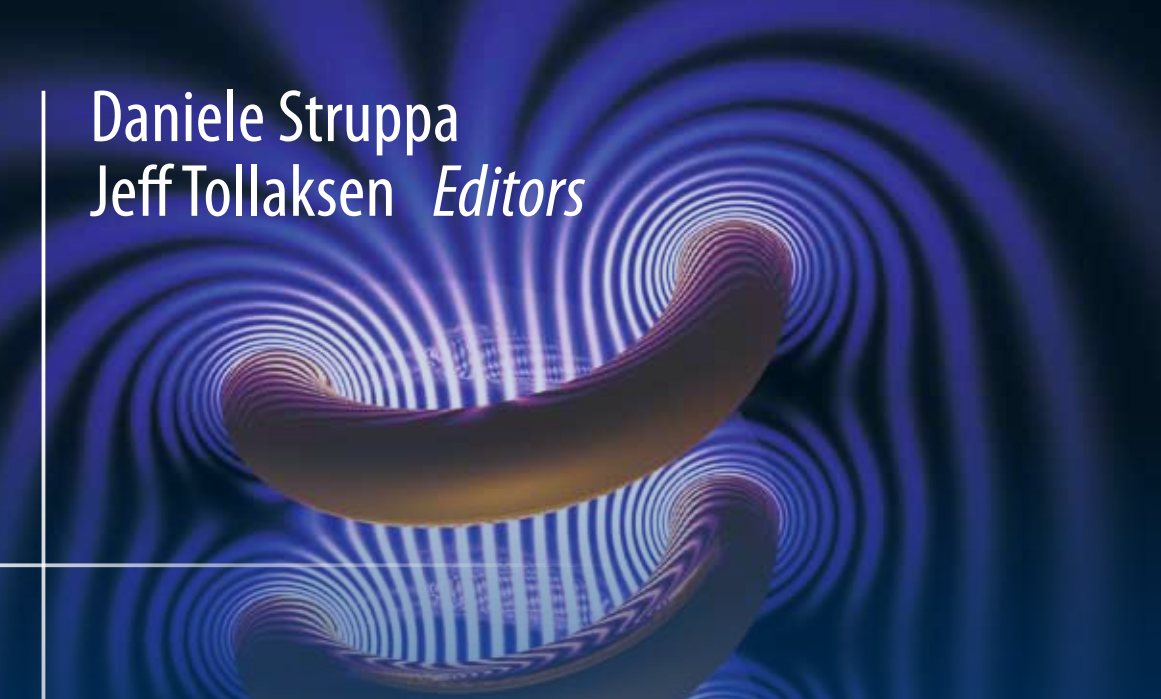

Quantum Theory: A Two-Time Success Story

Yakir Aharonov Festschrift

Springer

Chapter 21
Superoscillations, Endfire and Supergain

M.V. Berry

Abstract Superoscillatory functions vary faster than their fastest Fourier component. Here they are employed to give an alternative description and explicit recipe for creating endfire arrays with supergain, that is antennas with radiation patterns concentrated in an arbitrarily narrow angular range and of arbitrary form. Two examples are radiation patterns described by sinc and Gaussian functions. [*Editor's note*: for a video of the talk given by Prof. Berry (titled 'Weak Value Probabilities') at the Aharonov-80 conference in 2012 at Chapman University, see quantum.chapman.edu/talk-6.]

Dedicated to Yakir Aharonov on his 80th birthday: still quick, still deep, still subtle.

21.1 Introduction

The three elements of the title are connected. My aim here is to show how, in the hope of giving further insight into them.

A central ingredient of Aharonov's weak measurement scheme [1–3] is the concept of *superoscillations*. This is a property of band-limited functions: they can oscillate arbitrarily faster than their fastest Fourier component, over arbitrarily long intervals [4–6]. The price paid for this apparently paradoxical behaviour is that the functions are exponentially larger outside the superoscillatory region than in it.

An *endfire array* is an antenna in the form of a set of radiating sources arranged on a line (Fig. 21.1), the object of interest being the radiation pattern, that is, the angular distribution of wave intensity in the far field. It has been known at least since the 1940s [7–10] that if the array contains sufficiently many sources their strengths and phases can be so arranged that the radiation pattern is confined to an arbitrarily narrow region near the forward direction, even if the line containing all the sources

M.V. Berry (✉)
H H Wills Physics Laboratory, Tyndall Avenue, Bristol BS8 1TL, UK
e-mail: asymptotico@bristol.ac.uk

D.C. Struppa, J.M. Tollaksen (eds.), *Quantum Theory: A Two-Time Success Story*,
DOI 10.1007/978-88-470-5217-8_21,

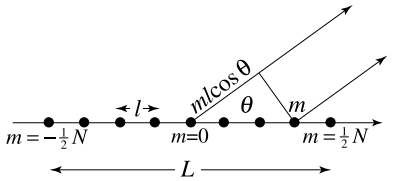

Fig. 21.1 Geometry and notation for endfire array with $N+1$ radiating sources

is arbitrarily smaller than the wavelength of the radiation. This phenomenon, apparently contradicting diffraction-theory folklore about resolving power, is *supergain* (also called superdirectivity). The concept, originating in radar physics, has been applied in optics [11–17].

Section 21.2 gives a general theory of supergain in terms of superoscillations, leading to a simple recipe for creating radiation patterns of any form, and connects this with the traditional explanation involving complex-variable theory. Section 21.3 gives two explicit examples: radiation patterns in the form of sinc functions and gaussians.

21.2 General Theory

Consider $N+1$ sources (N even) arranged uniformly on a line of length L (Fig. 21.1), so their spacing is $l = L/N$. The sources are point radiators of monochromatic scalar waves with wave length λ and wavenumber $k = 2\pi/\lambda$. With excitation amplitudes A_m, the far-field angular amplitude is

$$\begin{aligned}\psi(\theta) &= \sum_{m=-\frac{1}{2}N}^{\frac{1}{2}N} A_m \exp(-\mathrm{i}mkl\cos\theta + \mathrm{i}mkl) \\ &= \sum_{m=-\frac{1}{2}N}^{\frac{1}{2}N} A_m \exp\left(2\mathrm{i}mkl\sin^2\frac{1}{2}\theta\right). \end{aligned} \tag{21.1}$$

The phases $\mathrm{i}mkl$ have been included so that if all the A_m have the same phase the sources add coherently in the forward direction $\theta = 0$.

In this simplest case—all the A_m equal—the angular distribution is

$$A_m = \frac{1}{N+1}, \qquad \psi(\theta) = \frac{\sin(\frac{(N+1)}{N}kL\sin^2\frac{1}{2}\theta)}{(N+1)\sin(\frac{1}{N}kL\sin^2\frac{1}{2}\theta)} \approx \frac{\sin(kL\sin^2\frac{1}{2}\theta)}{kL\sin^2\frac{1}{2}\theta}. \tag{21.2}$$

The zero-amplitude directions ('cones of silence') are

$$\theta_n = 2\sin^{-1}\sqrt{\frac{\pi N n}{(N+1)kL}}, \quad 1 \le |n| \le \frac{kL}{\pi} = \frac{2L}{\lambda}. \tag{21.3}$$

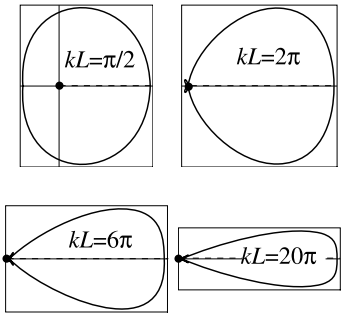

Fig. 21.2 Radiation patterns without supergain: polar plots of $\psi^2(\theta)$ given by (21.2) for the indicated values of kL. The *dots* indicate the origin $\psi^2(\theta)$, and the *dashed lines* indicate the forward direction $\theta = 0$

In particular, for large N, representing a line source, and $kL \gg 1$, the first zero is

$$\theta_1 \approx 2\sqrt{\frac{\pi}{kL}}, \tag{21.4}$$

as expected on the basis of the Rayleigh resolution criterion. As is well known, and as Fig. 21.2 illustrates, a narrow radiation pattern requires $kL \gg 1$.

However, by suitable choice of the strengths and phases of the amplitudes A_m it is possible to create radiation patterns as narrow as desired and indeed of arbitrary shape, even for $kL \ll 1$, i.e. $L \ll \lambda$—that is, to get supergain. To achieve supergain using superoscillatory functions, we first note that θ is not the natural variable, because $\psi(\theta)$ in (21.1), is not band-limited. This follows from the Bessel-Fourier relation

$$\exp(\mathrm{i}t\cos\theta) = \sum_{n=-\infty}^{\infty} i^n J_n(t)\exp(\mathrm{i}n\theta), \tag{21.5}$$

indicating that each term in (21.1) contains infinitely many angular Fourier components (i.e. angular momenta). However, defining the new variable x by

$$x \equiv kL\sin^2\frac{1}{2}\theta \tag{21.6}$$

gives the function

$$f(x) = \psi(\theta) = \sum_{m=-\frac{1}{2}N}^{\frac{1}{2}N} A_m \exp\left(\frac{2\mathrm{i}mx}{N}\right), \tag{21.7}$$

which is band-limited, with largest Fourier components proportional to $\exp(\pm\mathrm{i}x)$.

It is possible to create such functions with arbitrarily fast oscillations for small $|x|$, e.g.

$$f_{\text{super}}(x, a) \approx \exp(\mathrm{i}ax) \quad \big(a > 1, |x| \ll 1, N \gg 1\big). \tag{21.8}$$

The most familiar and much-studied [13] superoscillatory function, to be used extensively in the following, is

$$f_{\text{super}}(x) = \left(\cos\frac{x}{N} + \mathrm{i}a\sin\frac{x}{N}\right)^N. \tag{21.9}$$

This is periodic in x with period N. The small-x approximation $\exp(\mathrm{i}ax)$ oscillates rapidly but does not lead to a concentrated radiation pattern.

However, the simple procedure of integrating over the scale variable a, with a suitable weight function, enables any radiation pattern to be created, including the narrow ones corresponding to supergain. (This is a simplified variant, suggested to me by Professor Sandu Popescu, of a procedure previously used in an acoustic example in Sect. 4 of [4].) Let $g(a)$ be the Fourier transform of the desired angular amplitude, and construct the function

$$f(x) = \int_{-\infty}^{\infty} \mathrm{d}a f_{\text{super}}(x,a)g(a). \tag{21.10}$$

Then, for $|x| \ll 1$, $f(x)$ has, from (21.8), the desired form

$$f(x) \approx \int_{-\infty}^{\infty} \mathrm{d}a \exp(\mathrm{i}ax)g(a). \tag{21.11}$$

If $g(a)$ is even, as it will be in the examples in Sect. 21.3, $f(x)$ is a real function. The radiation pattern thus constructed is

$$\psi(\theta) = f\left(kL\sin^2\frac{1}{2}\theta\right). \tag{21.12}$$

As θ increases, this samples $f(x)$ from $x = 0$, corresponding to $\theta = 0$, to $x_{\max} = kL$, corresponding to the backward direction $\theta = \pi$. It is necessary to take N large enough to ensure that $x_{\max}$ lies in the superoscillatory interval where (21.8) applies, and this will be illustrated in Sect. 21.3. For $x > x_{\max}$ ('beyond backwards') the values of θ given by (21.6) would be complex.

The formula (21.12) represents the far field. We will see that the coefficients A_m, whose near-cancellation is responsible for supergain, take enormously large values (see Fig. 21.5 later). This implies that the wave intensity in the near field is correspondingly large, a phenomenon responsible for the well-known inefficiency of supergain antennas [8–10].

The conventional way of understanding supergain [7, 11] is via the complex variable

$$z = \exp\left(\frac{2\mathrm{i}x}{N}\right) = \exp\left(2\mathrm{i}kl\sin^2\frac{1}{2}\theta\right), \tag{21.13}$$

and the corresponding function

$$F(z) = \psi(\theta) = f(x) = \sum_{m=-\frac{1}{2}N}^{\frac{1}{2}N} A_m z^m. \tag{21.14}$$

Physical directions $-\pi \le \theta \le \pi$ (i.e. real θ, so $\sin^2(\theta/2) \le 1$) correspond to z on the unit circle and $|\arg z| \le 2kl$; for fixed L, this region shrinks towards the forward direction $z = 1$ as N increases. The zeros of $F(z)$ correspond to the cones of silence. In the simplest case discussed earlier, in which all A_m are in phase, we have

$$A_m = \frac{1}{N+1}, \qquad F(z) = \frac{(z^{N+1} - 1)}{(z-1)}, \tag{21.15}$$

whose zeros, uniformly distributed round the circle, are the $(N+1)$th roots of unity with $z = 1$ excluded. Supergain [11] corresponds to choosing the A_m so that the zeros, whose density increases with N, get concentrated into the physical region near $\arg z \ll 1$, that is, near the forward direction.

21.3 Examples: Sinc and Gaussian Radiation Patterns

21.3.1 Sinc Radiation Pattern

The simplest implementation of (21.10) is to make $g(a)$ constant on a finite interval and zero outside, that is, the Fourier transform of the sinc function. Then if the width of the interval is $2/w$, the function $f(x)$ given by (21.10) is

$$\begin{aligned} f(x, w) &= 2w \int_{-1/w}^{1/w} \mathrm{d}a f_{\text{super}}(x, a) \\ &= \frac{w}{(N+1)\sin\frac{x}{N}} \operatorname{Im}\left[\left(\cos\frac{x}{N} + \frac{\mathrm{i}}{w}\sin\frac{x}{N}\right)^{N+1}\right], \end{aligned} \tag{21.16}$$

and the radiation pattern is

$$\begin{aligned} \psi(\theta, w) = {} & \frac{w}{(N+1)\sin(kl\sin^2\frac{1}{2}\theta)} \\ & \times \operatorname{Im}\left[\left(\cos\left(kl\sin^2\frac{1}{2}\theta\right) + \frac{\mathrm{i}}{w}\sin\left(kl\sin^2\frac{1}{2}\theta\right)\right)^{N+1}\right]. \end{aligned} \tag{21.17}$$

When $w = 1$, this reproduces the radiation pattern of a line of coherently radiating sources (Eq. (21.2)). Otherwise, the analogous relation to (21.8) for small x and

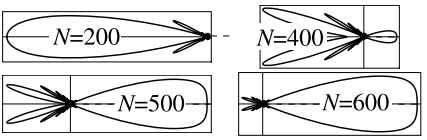

Fig. 21.3 Radiation patterns with supergain: polar plots of the sinc-based pattern $\psi^2(\theta)$ given by (21.17) for $kL = \pi/2$ (that is, an endfire array of length $L = \lambda/4$), and $w = 1/40$, for the indicated values of N. The *dots* indicate the origin $\psi = 0$, and the *dashed lines* indicate the forward direction $\theta = 0$

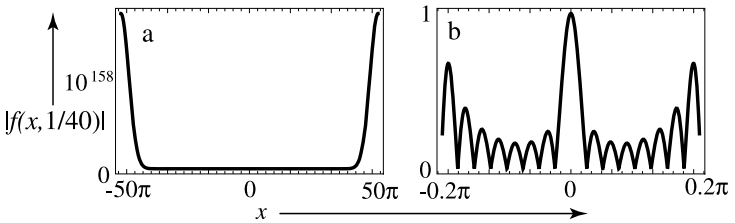

Fig. 21.4 Modulus of sinc-based function $|f(x, 1/40)|$ (Eq. (21.16)) for $N = 100$. (**a**) includes a complete period $|x| \le 50\pi$, and the sinc function near the origin is invisible; (**b**) includes the much smaller range $|x| \le 0.2\pi$, revealing the sinc

large N, namely

$$f(x, w) \approx \frac{\sin(x/w)}{(x/w)} \quad (x \ll 1, N \gg 1), \tag{21.18}$$

gives the approximate pattern

$$\psi(\theta, w) \approx \frac{w \sin(\frac{kL}{w} \sin^2 \frac{1}{2}\theta)}{kL \sin^2 \frac{1}{2}\theta}, \tag{21.19}$$

and hence supergain if $w < 1$. Figure 21.3 shows how supergain emerges as N increases, in the form of a narrow sinc radiation pattern for a short endfire array with length $L = \lambda/4$, and the small value $w = 1/40$.

When N is too small, the radiation is concentrated near the backward direction (e.g. for $N = 200$ in Fig. 21.3), because the limiting value $x_{\max} = kL$ sampled in $f(x, w)$ (Eq. (21.16)) is outside the region near $x = 0$ where the desired sinc function occurs, and instead lies in the exponentially large region beyond. Figure 21.4 illustrates the enormous disparity of values between these regions. For a quantitative understanding, we approximate $\psi(\theta)$ in (21.17) near $\theta = \pi$ and for $w < kL$:

$$\psi(\pi - \mu) \approx \left(\frac{w}{kL}\right) \sin\left(\frac{kL}{w}\left(1 - \frac{1}{4}\mu^2\right)\right) \times \exp\left(\frac{1}{2N}\left(\frac{kL}{w}\right)^2 (1 - w^2)\left(1 - \frac{1}{2}\mu^2\right)\right) \quad (\mu \ll 1). \tag{21.20}$$

This is exponentially large unless N exceeds a critical value N_c, which can be defined by requiring ψ^2, averaged over the oscillations near $\theta = \pi$, to equal the value $\psi(\theta = 0) = 1$. For $N > N_c$, the value near $\theta = \pi$ is exponentially small, corresponding to supergain. From (21.20),

$$N_c = \left(\frac{kL}{w}\right)^2 \frac{(1 - w^2)}{2\log\frac{\sqrt{2}kL}{w}}. \tag{21.21}$$

For the parameters of Fig. 21.3, $N_c = 440$, in fair agreement with the crossover to supergain.

The zeros of the radiation pattern are the directions

$$\theta_n = 2\sin^{-1}\sqrt{\frac{N}{kL}\tan^{-1}\left(w\tan\frac{n\pi}{N+1}\right)} \quad \left(1 \le |n| \le \frac{1}{2}N\right). \tag{21.22}$$

When $w = 1$ these cones of silence coincide with those of the equally phased array in (21.3). For small w they cluster closer to $\theta = 0$:

$$\theta_n \approx 2\sqrt{\frac{wn\pi}{kL}} \quad (w \ll 1, N \gg 1, n \ll N). \tag{21.23}$$

In terms of the variable z of conventional supergain theory, the zeros cluster closer to $z = 1$ on the unit circle.

The remarkable superdirectivity accomplished by superoscillation is a consequence of near-destructive interference between successive sources. For the pattern (21.17), the excitation amplitudes in (21.16) are

$$\begin{aligned} A_m(w) &= \frac{wN!}{2^{N+1}(\frac{1}{2}N+m)!(\frac{1}{2}N-m)!}\int_{-1/w}^{1/w} \mathrm{d}a\left(1-a^2\right)^{\frac{1}{2}N}\left(\frac{1+a}{1-a}\right)^m \\ &= \frac{wN!}{2^{\frac{1}{2}N-m+1}(\frac{1}{2}N-m)!} \\ &\quad \times \sum_{k=0}^{\frac{1}{2}N+m} \frac{(-1)^{\frac{1}{2}N-m}(\frac{1}{w}-1)^{\frac{1}{2}N-m+k+1} + (-1)^k(\frac{1}{w}+1)^{\frac{1}{2}N-m+k+1}}{2^k k!(\frac{1}{2}N+m-k)!(\frac{1}{2}N-m+k+1)}. \end{aligned} \tag{21.24}$$

(The sum can be expressed in terms of incomplete beta functions.) It is clear that $A_{-m}(w) = A_m(w)$, so we need study only $m \ge 0$. The simplest case is $w = 1$, for which $A_m(1) = 1/(N+1)$, corresponding to all sources in phase. For general w, the coefficients for the first few values of N are shown in Table 21.1.

The case of interest for supergain is $N \gg 1$, $w < 1$. Then Stirling's formula, and expansion of the integrands about their maxima, gives the asymptotics in terms of

Table 21.1 Coefficients $A_m(w)$ for $N = 2, 4, 6$

	$N=2$	$N=4$	$N=6$
$m=0$	$\frac{1}{6w^2}(-1+3w^2)$	$\frac{1}{40w^4}(3-10w^2+15w^4)$	$\frac{1}{112w^6}(-5+7w^2(3-5w^2+5w^4))$
$m=1$	$\frac{1}{12w^2}(1+3w^2)$	$\frac{1}{20w^4}(-1+5w^4)$	$\frac{1}{448w^6}(15+7w^2(-3-5w^2+15w^4))$
$m=2$		$\frac{1}{80w^4}(1+10w^2+5w^4)$	$\frac{1}{224w^6}(-3+7w^2(-3+5w^2+3w^4))$
$m=3$			$\frac{1}{448w^6}(1+7w^2(3+5w^2+w^4))$

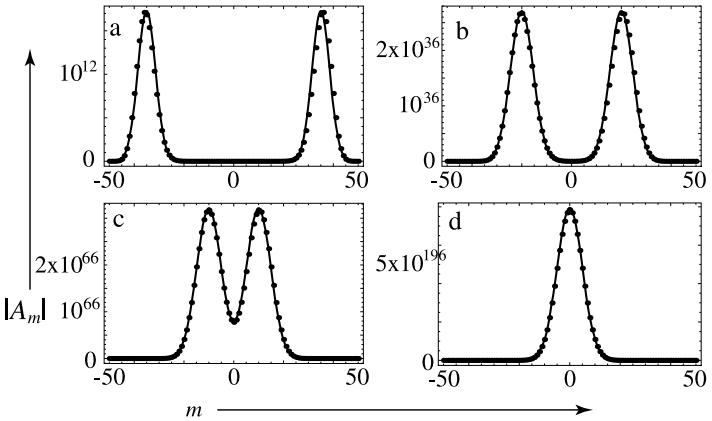

Fig. 21.5 Points: moduli of excitation coefficients A_m (Eq. (21.24)) for endfire array with $N+1 = 101$ radiating sources, for (**a**) $w = 0.7$, (**b**) $w = 0.4$, (**c**) $w = 0.2$, (**d**) $w = 0.01$. The *curves* show the approximation (21.25)

two Gaussians:

$$A_m(w) \approx \frac{(-1)^{\frac{1}{2}N+m}}{N^{\frac{3}{2}} w^N \sqrt{2\pi(1-w^2)}} \left[\exp\left(-\frac{2(m-\frac{1}{2}Nw)^2}{N(1-w^2)} \right) + \exp\left(-\frac{2(m+\frac{1}{2}Nw)^2}{N(1-w^2)} \right) \right]. \tag{21.25}$$

Note the alternating signs, indicating the near-cancellation responsible for supergain. Figure 21.5 shows the moduli of the coefficients. The agreement with the asymptotic formula appears excellent. However, using (21.25) instead of the exact coefficients in (21.1) leads to numerical instability and no hint of supergain: the interference is far too delicate to be captured by this lowest level of asymptotics. (For $w > 1$, the asymptotics is different: all amplitudes are in phase and there is no supergain.)

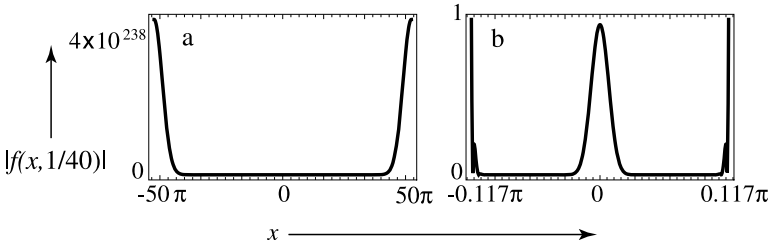

Fig. 21.6 Modulus of Gaussian-based function $|f(x, 1/40)|$ (Eq. (21.26)) for $N = 100$. (**a**) includes a complete period $|x| \leq 50\pi$, and the Gaussian near the origin is invisible; (**b**) includes the much smaller range $|x| \leq 0.117\pi$, revealing the Gaussian

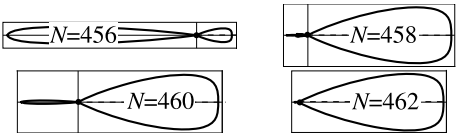

Fig. 21.7 As Fig. 21.3, for the Gaussian-based function generated from (21.26) using (21.12), with $w = 1/20$

21.3.2 Gaussian Radiation Pattern

The simplest example of a desired radiation pattern without zeros is the Gaussian, for which (21.10) is

$$\begin{aligned} f(x, w) &= \frac{w}{\sqrt{2\pi}} \int_{-\infty}^{\infty} \mathrm{d}a f_{\text{super}}(x, a) \exp\left(-\frac{1}{2}a^2 w^2\right) \\ &= \frac{\sin^N(x/N)}{(N+1)w^N 2^{N/2}} \left(\frac{w}{\sqrt{2}} \cot\left(\frac{x}{N}\right) H_{N+1}\left(\frac{w}{\sqrt{2}} \cot\left(\frac{x}{N}\right)\right)\right. \\ &\quad \left. - \frac{1}{2} H_{N+2}\left(\frac{w}{\sqrt{2}} \cot\left(\frac{x}{N}\right)\right)\right), \end{aligned} \tag{21.26}$$

where H denotes the Hermite polynomials. For small x, this gives the desired Gaussian with width w, and supergain for $w < 1$:

$$f(x, w) \approx \exp\left(-\frac{x^2}{2w^2}\right) \quad (x \ll 1). \tag{21.27}$$

(This limiting form, obvious from (21.11), can also be obtained from (21.26) by a large N resummation of the power series for the Hermite polynomials.) As in the case of the sinc pattern, enormous magnification is required to see the Gaussian, as Fig. 21.6 illustrates.

Some of the corresponding radiation patterns, obtained by the substitution (21.12), are shown in Fig. 21.7. In this case, the crossover to supergain as N increases is much more sensitive than in the sinc case (cf. Fig. 21.3).

Acknowledgements I thank Professor Stephen Lipson for introducing me to supergain, Professor Sandu Popescu for a helpful suggestion, Chapman University for generous hospitality while this work was begun, and the Leverhulme Trust for research support—and of course Yakir Aharonov for continuing inspiration.

References

1. Y. Aharonov, D.Z. Albert, L. Vaidman, How the result of a measurement of a component of the spin of a spin 1/2 particle can turn out to be 100. Phys. Rev. Lett. **60**, 1351–1354 (1988)
2. Y. Aharonov, D. Rohrlich, *Quantum Paradoxes: Quantum Theory for the Perplexed* (Wiley-VCH, Weinheim, 2005)
3. Y. Aharonov, S. Popescu, J. Tollaksen, A time-symmetric formulation of quantum mechanics. Phys. Today **63**(11), 27–33 (2010)
4. M.V. Berry, in *Faster than Fourier in Quantum Coherence and Reality; in Celebration of the 60th Birthday of Yakir Aharonov*, ed. by J.S. Anandan, J.L. Safko (World Scientific, Singapore, 1994), pp. 55–65
5. A. Kempf, P.J.S.G. Ferreira, Unusual properties of superoscillating particles. J. Phys. A **37**, 12067–12076 (2004)
6. Y. Aharonov, F. Colombo, I. Sabadini, D.C. Struppa, J. Tollaksen, Some mathematical properties of superoscillations. J. Phys. A **44**, 365304 (2011). (16 pp.)
7. S.A. Schelkunoff, A mathematical theory of linear arrays. Bell Syst. Tech. J. **22**, 80–107 (1943)
8. R.C. Hansen, Linear arrays, ed. by A.W. Rudge, K. Milne, A.D. Olver, P. Knight, *The Handbook of Antenna Design*, vol. 2 (Peter Peregrinus, London, 1983), pp. 1–134
9. H. Cox, R.M. Zeskind, T. Kooij, Practical supergain. IEEE Trans. Acoust. Speech Signal Process. **ASSP-34**, 393–398 (1986)
10. R.P. Haviland, Supergain antennas: possibilities and problems. IEEE Antennas Propag. Mag. **37**, 13–26 (1995)
11. G. Toraldo di Francia, SuperGain antennas and optical resolving power. Suppl. Nuovo Cim. **9**, 426–438 (1952)
12. I. Leiserson, S.G. Lipson, V. Sarafis, Superresolution in far-field imaging. Opt. Lett. **25**, 209–211 (2000)
13. M.V. Berry, S. Popescu, Evolution of quantum superoscillations, and optical superresolution without evanescent waves. J. Phys. A **39**, 6965–6977 (2006)
14. J. Lindberg, Mathematical concepts of optical superresolution. J. Opt. **14**, 083001 (2012). (23 pp.)
15. M.R. Dennis, A.C. Hamilton, J. Courtial, Superoscillation in speckle patterns. Opt. Lett. **33**, 2976–2978 (2008)
16. E.T.F. Rogers, J. Lindberg, T. Roy, S. Savo, J.E. Chad, M.R. Dennis, N.I. Zheludev, A superoscillatory lens optical microscope for subwavelength imaging. Nat. Mater. **11**, 432–435 (2012)
17. M.V. Berry, M.R. Dennis, Natural superoscillations in monochromatic waves in D dimensions. J. Phys. A **42**, 022003 (2009)

Daniele Struppa · Jeff Tollaksen *Editors*

Quantum Theory: A Two-Time Success Story

Yakir Aharonov Festschrift

Yakir Aharonov is one of the leading figures in the foundations of quantum physics. His contributions range from the celebrated Aharonov-Bohm effect (1959), to the more recent theory of weak measurements (whose experimental confirmations were recently ranked as the two most important results of physics in 2011). This volume will contain 27 original articles, contributed by the most important names in quantum physics, in honor of Aharonov's 80-th birthday.

Sections include "Quantum mechanics and reality," with contributions from Nobel Laureates David Gross and Sir Anthony Leggett and Yakir Aharonov, S. Popescu and J. Tollaksen; "Building blocks of Nature" with contributions from Francois Englert (co-proposer of the scalar boson along with Peter Higgs); "Time and Cosmology" with contributions from Leonard Susskind, P.C.W. Davies and James Hartle; "Universe as a Wavefunction," with contributions from Phil Pearle, Sean Carroll and David Albert; "Nonlocality," with contributions from Nicolas Gisin, Daniel Rohrlich, Ray Chiao and Lev Vaidman; and finishing with multiple sections on weak values with contributions from A. Jordan, A. Botero, A.D. Parks, L. Johansen, F. Colombo, I. Sabadini, D.C. Struppa, M.V. Berry, B. Reznik, N. Turok, G.A.D. Briggs, Y. Gefen, P. Kwiat, and A. Pines, among others.

Physics

ISBN 978-88-470-5216-1

9 788847 052161

springer.com